INTEGRAL AND SPECTRAL CHARACTERISTICS OF ATON STATIONARY PLASMA THRUSTER OPERATING ON KRYPTON AND XENON

A.I.Bugrova, A.I.Morozov*, A.S.Lipatov, A.M.Bishaev, V.K.Kharchevnikov, M.V.Kozintseva.

Moscow Institute of Radio Engineering, Electronics and Automation (Technical University), Laboratory of Plasmaoptics, prosp. Vernadskogo, 78, Moscow, Russia, 119454.
Tel.: (095) – 434-86-22
Fax: (095) – 434-86-65
E-mail: bugrova@mirea.ru

*Russian Scientific Center "Kurchatov Institute", Kurchatov sq., 1, Moscow, Russia, 123182.
Tel.: (095) – 196-77-55
Fax: (095) – 434-86-65
E-mail: bugrova@mirea.ru

Abstract

The integral characteristics of an ATON [1] stationary plasma thruster operating on xenon and krypton are investigated. It is shown that, with krypton, the thrust at the same mass flow rate of the working gas is greater and the efficiency is somewhat lower than those with xenon. An efficiency of ~60% was achieved with krypton for the specific impulse attaining 3000 s. The jet divergence is ~±22 ° for krypton and ~±11 ° for xenon. The radiative characteristics of Krypton plasma of the stationary plasma thruster of ATON type have been studied on the basis of the measurements of the absolute intensities of the spectral lines in the waves lengths band 0.24 mcm< λ <1.0 mcm. It has been obtained, that the visual band is the dominant one, and that the single charged ions KrII are the main radiating particles. It has been shown that the losses onto the radiation in the channel in this band are about 14W. There are treated the features of the population and the depopulation of atoms KrI and ions KrII levels due to radiative transitions in the ionization zone.

1.Experimental Set Up

The studies of integral and local parameters were carried out in an ATON SPT [1] of the A-3 type, which is shown schematically on Fig. 1. The inner diameter of the outer insulator was 60 mm, the channel length was 24 mm, and the gap width was b =12 mm. The experiments were performed in the input power range $W \le 2.0$ kW. With each working gas, the accelerator operated under optimum conditions, which were characterized by the minimum discharge current. The pressure in the chamber was 10^{-4} torr.

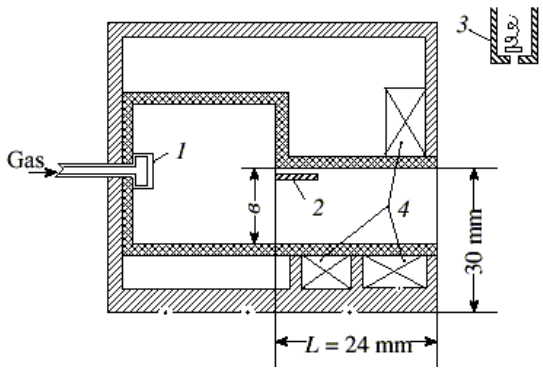

Fig. 1. Schematic of an A-3 SPT: (1) – gas distributor, (2) - anode, (3) – cathode, and (4) – magnetic coils.

All spectral measurements have been carried out at the same thruster operating mode: Kr mass flow rate through gas-distributor was $\dot{m}_{anode} = 2.0 mg/s$, Kr mass flow rate through the cathode was $\dot{m}_{cathode} = 0.5 mg/s$, discharge voltage - U_d=300 V, discharge current - J_d=3.0 A.

In order to obtain spectra from the thruster channel, longitudinal (along thruster axis) slit, length 20 mm and height 1.5 mm, was cut in the external insulator of the channel.

Plasma radiation from the channel (or the jet) of the thruster through quartz window in the vacuum chamber wall hit quartz condenser and was focused onto the entrance slit of the monochromator MDR - 23 with a scan of a spectrum. As the calibrating source for the change to the absolute intensities, the strip tungsten lamp SIRSH-8,5–200-1 with uviol input window has been used.

2. Scaling Law

According to the scaling law [2,3], an accelerator operating with the same working gas, but with different mass flow rates operates in the same (with respect to the global characteristics) mode if the value of the parameter α,

$$\alpha \equiv \frac{\dot{m}}{S} \cdot b \qquad (1)$$

is the same. Here, $\dot{m}$ is the mass flow rate of the working gas, S is the channel cross-sectional area, and b is the channel width.

As it was shown in [2, 3], the parameter α can be rewritten in the form

$$\alpha = \frac{1}{\sqrt{\Lambda_*}} \cdot \left(\frac{\varepsilon \cdot T_0}{\beta^2} \right)^{1/2} \qquad (2)$$

where $\Lambda_* = \Lambda \cdot \delta$; $\Lambda = \lambda_{ion}/L$ is the dimensionless ionization length; L is the effective channel length over which the electric field is sufficiently high; $\delta = \varepsilon/(eU_d)$, ε is the ion energy cost, which is close to the quantity ΔU which determines the energy spent on ionization and other losses; U_d is the discharge voltage; T_0 is the temperature of the working gas atoms at the inlet into the SPT channel; and $\beta(T_e, A) = \langle \sigma V \rangle$ is the ionization coefficient, which depends on the electron temperature T_e and the sort of the working gas. However, expression (2) is inconvenient to use. For this reason, we clarify its physical meaning and put it into a practically usable form [5]. Indeed, it follows from expressions (1) and (2) that

$$\left(\frac{\dot{m}}{S} b \right)^2 \sim \frac{eU_d}{\beta^2} T_0 = const \qquad (3)$$

Hence, the mass flow rate of the working gas is a universal function of the main accelerator parameters U_d, b, S and T_0. Apparently, this conclusion is accurate to within β. Since β depends only slightly on the properties of the working gas and, moreover, the electron energy distribution function and its time evolution in the accelerator channel are not known with certainty, the conclusion about the equality of the mass flow rates for thrusters that have the same sizes, but operate with different working gases is accurate to a factor of 2.

3. Integral Parameters of the A-3 model

Figure 2a shows the static current-voltage characteristics of a model plasma accelerator operating with Xe and Kr. The characteristics were obtained under the optimum (with respect to the magnetic field) operating conditions at the same mass flow rate $\dot{m}$ = 2.3 mg/s [6]. It is seen from the figure that, in the voltage range 250 V ≤ U_d ≤ 400 V for Xe and 300 V ≤ U_d ≤ 500 V for Kr, the discharge current depends only slightly on the voltage, which indicates the high degree of ionization of the working gas.

For Xe in the above voltage range, the discharge current either is equal to the mass current $J_{\dot{m}} = \frac{e}{M} \cdot \dot{m}$ expressed in amperes or somewhat exceeds the value of $J_{\dot{m}}$ because of the presence of a "transit" electron current and a certain fraction of doubly charged ions (10-12%).

When Kr is used as a working gas, the discharge current is substantially higher than the mass current. This may be

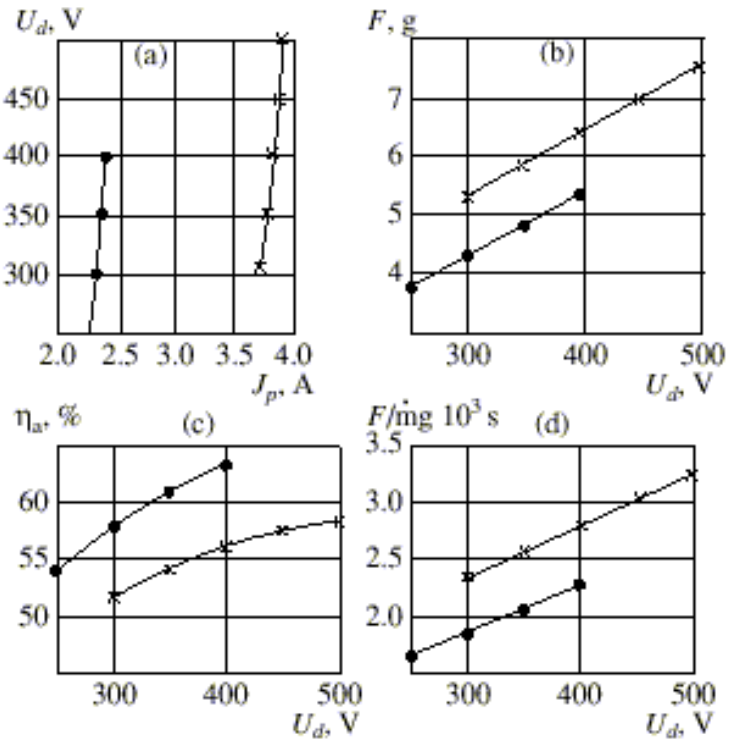

Fig. 2.
Current–voltage characteristics of the discharge (a) and the dependencies of the thrust (b), efficiency (c), and specific impulse (d) on the discharge voltage at =2.3 mg/s for Kr (crosses) and Xe (circles).

attributed to the worse focusing of the plasma flow in the channel as compared to the case of Xe and, consequently, to the different near-wall conductivity, which affects the discharge current [4].

When operating with both of these gases, the discharge-current fluctuations in the frequency range 1-300 kHz are $\tilde{J}/\bar{J} \le 0.1-0.2$.

Figure 2b shows the result of the thrust measurements at the mass flow rate $\dot{m}$ =2.3 mg/s for Xe and Kr. It can be seen from the figures that, at the same mass flow rate, the thrust for Kr is greater than for Xe. This is explained by the fact that, at the same mass flow rate and a sufficiently high degree of ionization of the working gas (see Fig. 2a, illustrating the current-voltage characteristic of the discharge), the number of the created ions is inversely proportional to the atomic mass, and, consequently, the number of Kr ions producing the thrust is greater than the number of Xe ions.

Although the thrust for Kr is higher than for Xe, the thruster efficiency for Kr is lower (Fig. 2c). This is a consequence of the fact that the mass current for Kr is substantially higher than for Xe, whereas the ionization losses for Xe are lower.

Figure 2d shows the specific impulse as a function of the discharge voltage for Xe and Kr at the same mass flow rates. It can be seen from the figure that the specific impulse of a thruster operating with Kr is substantially higher, which can be attributed to the higher velocity of the plasma flow.

Table 1

$\dot{m}_a$, mg/s	1,5	2	2,3	2,5
U_d, V	400	400	400	400
J_d, A	2,5	3,3	3,9	4,2
F, g	3,6	5,3	6,4	7,25
η, %	42	51	55	60
$F/\dot{m}$, s	2400	2650	2780	2900

As the voltage increases from 300 to 500 V, the thruster efficiency increases from 52 to 58%; the specific impulse at 500 V attains 3240 s. Table 1 present the global characteristics of a thruster operating with Kr for the same voltage and different mass flow rates. Thus, for U_d=400 V and the mass flow rate $\dot{m}$ =2.5 mg/s, the thruster efficiency attains 60% for a specific impulse of the 2900 s.

4.Local Plasma Parameters in the Channel and Jet of the Accelerator

The local plasma parameters in the channel and jet of the accelerator were measured with a plane face probe. The probe size was chosen such that the probe only slightly perturbed the plasma. For this reason, the measurements in the channel were performed with a face probe with a working surface area of S=0.2 mm^2.

The local plasma parameters in the accelerator channel were measured with the help of five wall probes located at distances of 5,15, 20, and 25 mm from anode. In the plasma jet, the measurements were performed with a similar probe that could be displaced in the longitudinal and radial directions (0≤z≤30 cm, o≤r≤20 cm).

Figure 3.1 shows the axial profiles of the plasma potential (a), electron temperature (b), and electron density (c) in the channels of accelerators operating with Xe and Kr at $\dot{m} = 2mg/s$ and U_d=300 V. It is seen that, for Kr, the electron temperature in the ionization region is lower and the electron density n_e is higher than for Xe. The latter may be explained by the fact that, at the same mass flow rates, the number of Kr atoms entering the accelerator channel is greater than that of Xe atoms by a factor of nearly 1.6, whereas the cross section for electron-impact ionization for Xe in the given electron energy range is greater than for Kr by factor of 1.5.

It can also be seen that, for Kr, the potential difference, accelerating the ions, is somewhat lower than for Xe. In the case of Xe, the plasma potential remains constant at a distance of 12-13 mm from the anode and then drops. This means that, in this case, the electric field occupies a region of length ~13 mm. For Kr, the potential is constant at a distance of 10-11 mm from anode and then drops. In this case, the electric field occupies a region of length ~15 mm.

The electron temperature distribution in both cases is bell-shaped. The full width at half-maximum corresponds to the size of the region occupied by the electric field.

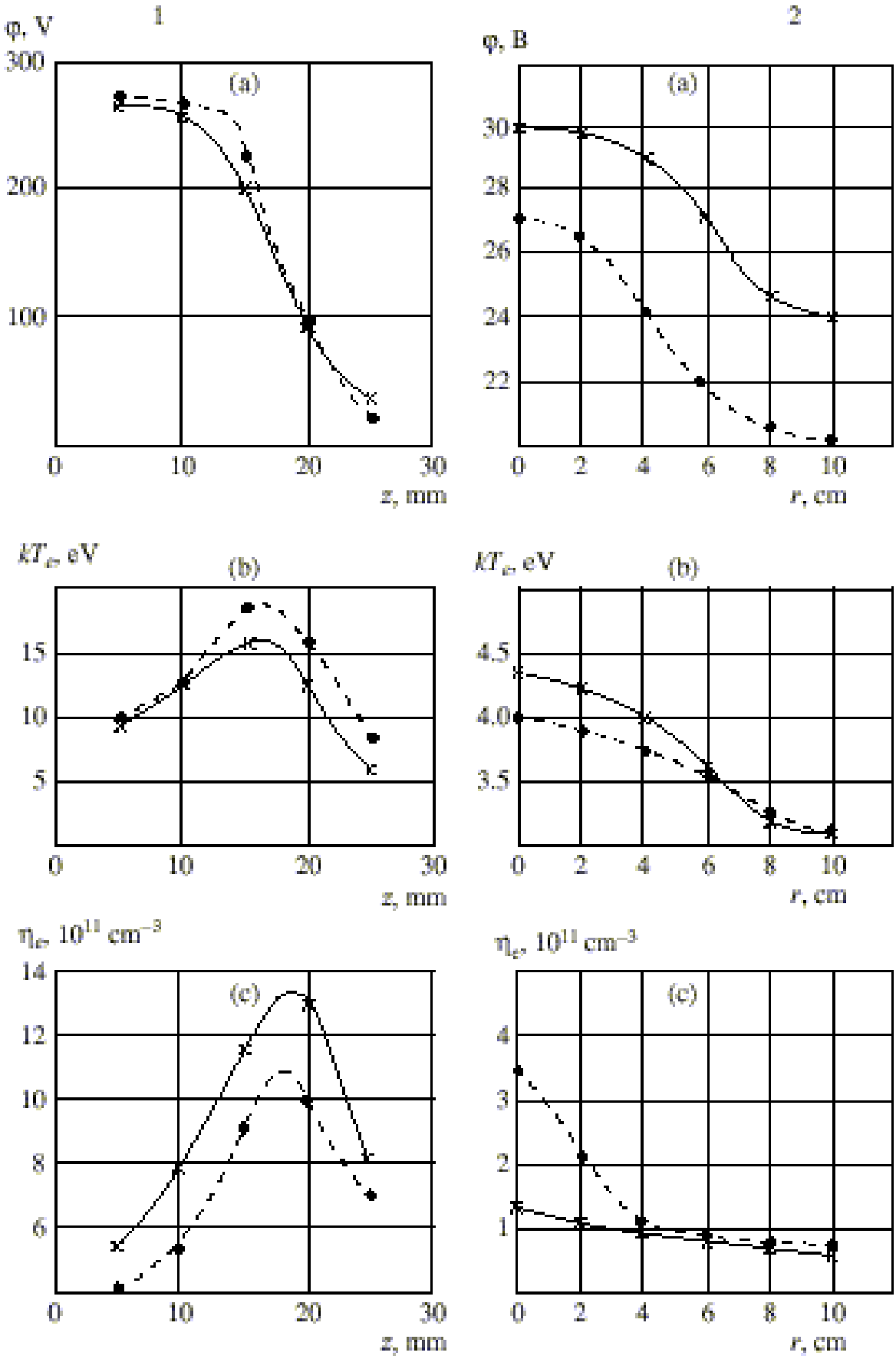

Fig. 3. Distributions of the plasma potential (a), electron temperature (b), and electron density (c) in the channel (I) and in the jet (II) behind the outlet of the accelerator at = 2 mg/s and U_d = 300 V for Kr (crosses) and Xe (circles); the anode and the accelerator outlet are located at z = 0 and 25 mm, respectively.

Figure 3.2. shows the radial profiles of the plasma potential (a), electron temperature (b), and electron density (c) in the accelerator jet at a distance of z=30 cm from the outlet in accelerators operating with Xe and Kr at $\dot{m}$ =2 mg/s and U_d=300 V. A comparison of the local parameters of accelerators operating with Kr and Xe shows that the electric potential and the electron temperature at the jet axis (r=0) are higher for Kr. This means that, for Kr, these parameters decrease more slowly with distance from the outlet.

The divergence of the plasma jet was measured with a double electric probe. The probe was located at a distance of z=20 cm from the outlet of the accelerator and could be displaces in the radial direction. For every operating regime, we measured the profile of the ion current onto the probe. These curves were then used to calculate the half-angle of the jet divergence for Kr. The value of $\alpha/2$ was determined from the condition that 95% of the ion flow has fallen within the cone with the vertex angel α. The data on $\alpha/2$ are presented in Table 2.

Table 2

$\dot{m}_a$, mg/s	2	2	2,3	2,3
U_d, V	300	400	300	400
$\pm\alpha/2$	27^0	25^0	24^0	22^0

It is seen from the table that the half-angle of the jet divergence varies from $\pm22^0$ to $\pm27^0$, depending on the operating conditions. This value is substantially greater than that for an accelerator operating with Xe, where the half-angle of the jet divergence is $\pm11^0$.

5. Spectral Characteristics

As it is known from the investigation of the physical processes in the thruster, operating on Xe [1], the ionization field, where the most intensive ions burning takes place, and the thruster exit, from which already formed ions flow goes out, are the most interesting through the physical meaning plasma fields. Therefore the spectra under the thruster operation on Kr have been obtained:

- in the thruster channel from the cross-section z=15mm from the anode (ionization zone);
- from the thruster outlet in the jet (z=24mm from the anode).

The overall view of spectrum, obtained from the ionization field of the channel, is shown on fig.4. As one may see from the figure, the most intensive radiation is concentrated in the blue-violet spectrum band and is under an obligation to ions, and only some powerful atom lines are in IR band.

Summarizing absolute intensities, we've obtained the distribution of the power, radiated from the plasma volume unit in all directions, onto the waves lengths bands [7]. Corresponding diagram is represented on fig.5. One may see from the figure, that the visual band provides the biggest contribution into the channel plasma radiation: 2/3 of the total radiation power of the investigated band falls at it. Accordingly about 1/5 of the total power falls at UV, and approximately 1/10 part – at IR band of spectrum.

It is interesting to trace the distribution onto particles of the total energy, radiated in the band λ=0.24÷1.0 mcm. It is represented on the diagram 6. As it is seen from the figure, the radiation of the single charged ions Kr II is the dominant: it accounts for over 3/4 of the total energy of this band. More over, 1/3 of the total emitted energy falls at 12 powerful ion lines. These are the lines, which wave lengths are in the band 3718 $\mathring{A}$ -4475 $\mathring{A}$, and the most powerful line is the line with wave length 4355 $\mathring{A}$ (~$1{,}4\cdot10^4$ Вт/м^3). The share of neutral atoms is about 1/5 of the radiated power. The contribution of double charged ions KrIII emission is lesser than a percent, and about 2% of the radiation energy falls at impurities.

The overall view of spectrum, obtained from the exit of A-3 model, is shown on fig.7. Comparing figs.4 and 7, one may say [7], that:

- as in the channel, the main radiation contribution falls at near UV and blue-violet field of spectrum;
- in comparison with spectrum from the channel, IR band contribution has fallen off, and therefore atoms lines contribution has fallen too.

The modification of the radiation spectrum composition is confirmed by the correspondent calculations. So, summing the absolute intensities of lines we've obtained the distribution of the power, emitted at the exit, onto the waves lengths bands. It is shown on the diagram 8. Comparing it with the analogous diagram for the ionization zone (fig.5), we see that:

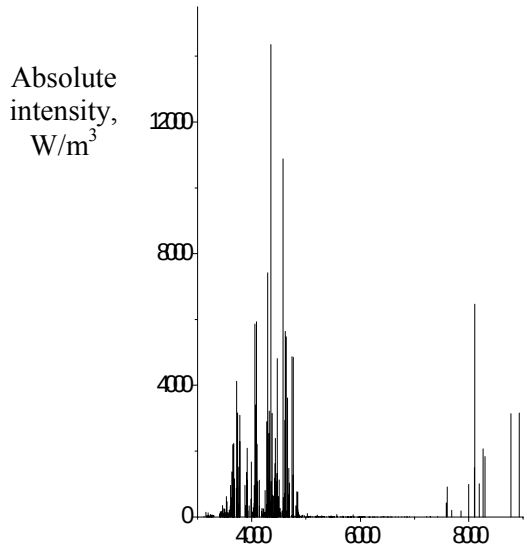

Fig.4. Spectrum from Ionization Region of A-3, operating on Kr

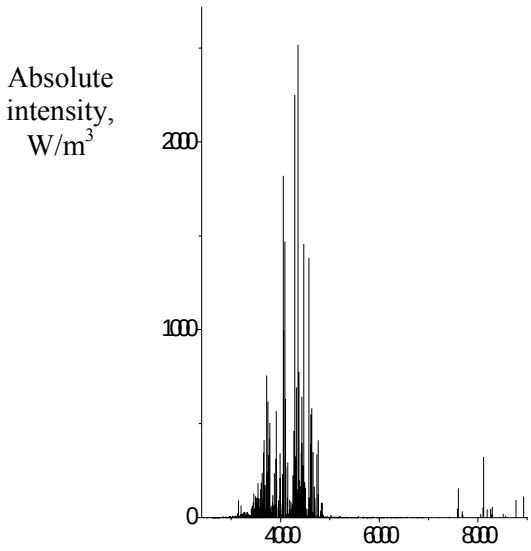

Fig.7. Spectrum on A-3 Exit on Kr

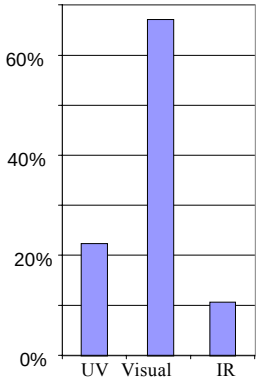

Fig.5. Radiation Energy Distribution onto Bands in Ionization Region of A-3 Channel on Kr

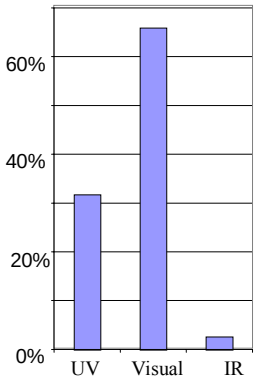

Fig. 8. Radiation Energy Distribution onto Bands at A-3 Exit on Kr

- at the exit, as in the ionization zone, the visible band is the dominant: for both cases it occupies ~2/3 of the total radiation power;
- UV band contribution at the exit has increased up to ~1/3;
- IR band contribution at the exit has decreased in 4 times (from 10,5% to 2,5%).

The distribution on particles of the total energy, radiated at the exit in the band λ=0.24÷1.0 mcm, is shown on the diagram 9. Comparing it with the analogous diagram, plotted for ionization field, we see, that:

- the radiation of the single charged ions KrII is the dominant both at the exit and in the channel: about 80% of the total radiated energy falls at it;
- the contribution of atoms KrI radiation at the exit has decreased approximately in 1,5 times and has been about 13%;
- the contribution of double charged ions KrIII has increased at the outlet, in comparison with ionization zone, in 3 times and has become equal to ~3%;

- the impurities contribution in the total radiation has increased at the exit in comparison with the ionization zone and has exceeded 3%.

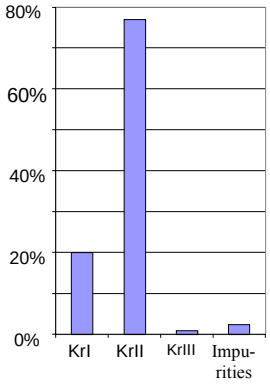

Fig.6. Radiation Energy Distribution onto Particles in Ionization Region of A-3 Channel on Kr

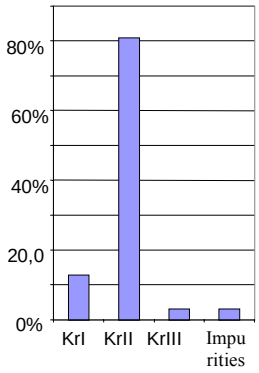

Fig.9. Radiation Energy Distribution onto Particles at A-3 Exit on Kr.

Using the data of the spectral measurements in the band λ=0.24÷1.0 mcm, the picture of the radiative transitions of atom KrI has been plotted in the ionization zone of the thruster [8]. According to the plotted scheme the depopulation of all excited states of atoms owing to radiation leads finally to the transition of atoms either to resonance, or to metastable level. As a result, one part of atoms, when transiting to the ground state, create VUV radiation in the channel; other atoms, being metastable, carry the radiation away into plasma jet.

Using the data of the spectral measurements in the band λ=0.24÷1.0 mcm, the picture of the radiative transitions of ion KrII has been plotted in the ionization zone of the thruster [8]. The feature of the given chart is in the fact, that owing to radiative transitions of ions KrII only resonance ion levels are occupied. It means, that:

- metastables of KrII, possibly, are occupied mainly through an electron shock or other mechanisms, excluding cascades;
- excited in the ionization zone onto the high terms ions KrII "throw off" their excitation in the channel, dropping back to the ground state owing to radiative transitions in the visual and VUV bands through the one of the resonance levels.

Proceeding from the values of the absolute intensities one may estimate the power, carried away by the plasma radiation of the channel. Summing absolute intensities, we obtain, that $1m^3$ of plasma in the channel ionization zone per 1 second emits in all directions $\sim 2 \cdot 10^5$Watt within the band λ=0.24÷1.0 mcm. As it was obtained experimentally the visual band is the dominant one at the exit and in the ionization zone of the thruster under its operating on Kr. Therefore one may approximately consider, that the distribution of the radiated energy along the channel is close to the distribution of the intensity of the lines of the visual band. We had the data about the behavior of 5 atom lines of the visual band along the channel. All of them have approximately the same behavior. Then, considering that the distribution of the radiated energy along the channel is in the same manner as the distribution of the intensity of line 4376KrI, we obtain, that the power, emitted within the range (0,24 - 1,0) mcm in the channel of A-3, operating on Kr in the mode U_d=300V and I_d=3A, is about 14W (i.e. approximately 1,6% of the input power). Thus, the losses by radiation in the channel under thruster operating on Kr exceed in 3,5 times the losses by radiation under thruster operating on Xe under the close in power mode (U_d=350V and I_d=2,0A).

It is necessary also to note, that the jet under the thruster operation on Kr is sufficiently powerful source of the radiation, so, under the rough estimations, the losses by the radiation in the jet are only in few times lesser the losses by the radiation in the channel.

Thus the total losses by the radiation in the channel and the jet of A-3 thruster on Kr within the band λ=0.24÷1.0 mcm are, according to undervalued estimation, about ~20W, i.e. about 2,2% of the input power.

5.Conclusion.

The experiment has shown that, in accordance with the scaling law, a stable high-performance SPT operation can be achieved with Kr. In this case, the following effects have been observed:

(I) At the same (as for Xe) mass flow rate of the working gas, the specific impulse (thrust) is greater than with Xe.

(II) The efficiency of a thruster operating with Kr is lower than operating with Xe. This is explained by the higher energy cost of an ion.

(III) The jet divergence obtained with Kr is greater than with Xe. However, this disadvantage stems apparently from the nonoptimized operation of the out-put section of the source (the outlet-cathode region).

Using the experimentally obtained composition of Krypton plasma radiation and the values of the absolute intensities of the emission lines, the scheme of the population and depopulation of the energy levels of atoms KrI and ions KrII has been rebuild under the thruster operation on Kr. These data will allow to choice the most adequate for the given experimental conditions plasma model and using the modern programs block to predict the change in the plasma behavior under the change of the parameters of the accelerator operation mode.

6.Acknowledgement.

Authors thank all members of MIREA "Physical plasmaoptics" laboratory for the experimental assistance.

The work has been carried out under financial support of INTAS-99-1225.

References

1. A. I. Morozov, A. I. Bugrova, A. V. Desyatskov, *et al*. // Fiz. Plazmy, **v. 23**, №7, p.p.635-645 (1997) [Plasma Phys. Rep., **v. 23**, p.p.587-599 (1997)].
2. A. I. Morozov and I. V. Mel'nikov // Zh. Tekh. Fiz., **v.44**, p.544 (1974) [Tech. Phys.,v.**1**9, p.340 (1974)].
3. A. I. Bugrova, N. A. Maslennikov, and A. I. Morozov // Zh. Tekh. Phys., **v. 61** (6), p.45 (1991) [Tech. Phys., **v. 36**, p.612 (1998)].
4. A. I. Morozov, *Physical Concepts of Electrical-Propulsion Engines* (Atomizdat, Moscow, 1978).
5. A. I. Bugrova, A.S. Lipatov, A. I. Morozov, *et al*. // Pis'ma v Zh. Tekh. Phys., 2002y., **v.28**, №19, p.p.56-61[Tech. Phys. Lett., **v. 28** (2002)].
6. A. I. Bugrova, A.S. Lipatov, A. I. Morozov, *et al*. // Fiz. Plazmy, 2002y., **v. 28**, №12, p.p.1118-1123 [Plasma Phys. Rep., **v. 28**, p.p.1032-1037 (2002)].
7. A.I.Bugrova, A.V.Desyatskov, M.V.Kozintseva, *et al*.// "Molodie uchenie-2002". Proceedings of the International Science-Technical School-Conference "Young scientists – to science, technologies and professional education", 1-4 of October 2002y., Moscow, Russia.-M.:MIREA 2002, p.p. 45-48.
8. A.M.Bishaev, S.V.Baranov, M.V.Kozintseva, *et al*.// "Molodie uchenie-2002". Proceedings of the International Science-Technical School-Conference "Young scientists – to science, technologies and professional education", 1-4 of October 2002y., Moscow, Russia.-M.:MIREA 2002, p.p. 40-44.